SUMMARY OF MASTCAM-Z VISIBLE TO NEAR INFRARED (VNIR) MULTISPECTRAL OBSERVATIONS FROM PERSEVERANCE'S MISSION IN JEZERO CRATER, MARS. M. S. Rice[1], J. R. Johnson[2], C. C. Million[3], M. St. Clair[3], B. N. Horgan[4], A. Vaughan[5], J. I. Núñez[2], B. Garczynski[4], S. Curtis[1], K. M. Kinch[6], A. Hayes[7] and J. F. Bell[5], [1]Western Washington Univ., Bellingham, WA, USA (melissa.rice@wwu.edu), [2]Johns Hopkins University Applied Physics Laboratory, [3]Million Concepts, [4]Purdue Univ., [5]Arizona State Univ., [6]Univ. Copenhagen, Denmark, [7]Cornell Univ.

Introduction: In its first year of exploration, NASA's Mars-2020 Perseverance rover has traversed multiple units in the floor of Jezero crater, including the cratered floor fractured rough (Cf-fr) and the southern portion of the Séítah region within the older, rougher Cf-f1. Within these units, Perseverance has encountered rocks with a diversity of textures, morphologies, surface coatings, colors, and spectral properties. Understanding the full variety rock and soil characteristics, and mapping their occurrences across the rover's traverse, will be key to interpreting the deposition and subsequent modification of the crater floor units. Perseverance has multiple high-resolution imaging and spectroscopic instruments among its payload; of these, the Mastcam-Z instrument is unique in that it can quickly acquire spectral information over broad spatial areas. Here, we summarize the spectral diversity observed in Mastcam-Z multispectral observations to date.

Mastcam-Z Data: Mastcam-Z is a pair of multispectral, stereoscopic zoom-lens cameras that provide broadband red/green/blue (RGB), narrowband visible to near-infrared color (VNIR, 440-1020 nm wavelength range), and direct solar imaging capability [1]. The 4:1 zoom lenses provide continuously variable fields of view (FOVs) ranging from ~5º to ~23º, and will allow Mastcam-Z to resolve features ~1 mm in size in the near field. We used near-simultaneous observations of the Mastcam-Z calibration targets [2] with pre-flight calibration coefficients [3] to calibrate Mastcam-Z surface observations to I/F. Spectra are the converted to reflectance factor (R^*) by dividing by the cosine of the solar incidence angle.

From inspections of natural color, enhanced color, decorrelation stretch and band parameter images from each observation [4], we selected regions of interest (ROIs) from which to extract a representative set of R^* spectra from each multispectral observation. We classified each spectrum with feature type (e.g., rock, soil), surface description (e.g., dusty natural surface, abrasion patch, bedform), morphology (e.g., layered, paver), and extensive metadata from the image headers. As of sol 280, Mastcam-Z has acquired 160 full-filter observations of geologic targets, including 226 unique pointings of the surface. From these, we have compiled a database of 1463 spectra of geologic surface materials encountered to date.

Spectral Classes: We used Principal Component Analysis (PCA), parameter plots [4] and visual inspections of the full spectral dataset to identify a set of geologically-meaningful Mastcam-Z classes. We define five major spectral types that represent the high-level spectral variability of the dataset:

1. Neutral/Dusty Spectra are characterized by strong blue-to-red slopes in visible wavelengths and flat near-infrared profiles, where no mafic signatures are observed (e.g., Fig. 1). These spectra are common to spectrally-neutral, dark surfaces covered with thin layers of dust (nanophase ferric oxide).

2. Ferric Dust Coatings Spectra are characterized by strong blue-to-red slopes in visible wavelengths, 528 nm absorption bands, and downturns at 1022 nm. These spectra have only been associated with thick dust coatings on rock surfaces. The 1022 nm downturn is consistent with an absorption near ~1000 nm due to H_2O and/or OH in some hydrated minerals. Although viewing geometry may influence this feature (as observed for dust by MER Spirit's Pancam in Gusev crater [5]), photometric studies of dust deposits at Opportunity at Meridiani Planum suggest the downturn can be real [6].

3. Pyroxene-like Spectra are characterized by broad absorptions centered at 908 nm and reflectance peaks at 754 nm. These spectra are associated with dark-toned rocks and soils across all regions of the traverse. While most spectra are more consistent with orthopyroxenes, there is considerable band center variability between 866-939 nm that indicates mixtures of clinopyroxenes and orthopyroxenes are also likely.

A broad, weak 908 nm band is also seen in purple-hued coatings on some rock surfaces [7] (e.g., targets Hedgehog, Rochette, Lance and Estoubion). These occurrences have strong 528 nm absorptions and may be more consistent with oxyhydroxides.

4. Hematite-like Spectra have strong 528 nm and 866 nm absorptions, and strongly positive NIR slopes, consistent with fine-grained, red hematite. These spectra have mostly been seen in "paver" rock morphologies within abraded patches (e.g., at target Guillaumes) and other dust-removed surfaces (e.g., the SuperCam LIBS depth profile target Nataani). We see some rocks with these spectra within Séítah, most likely associated with weathering rinds and/or coatings.

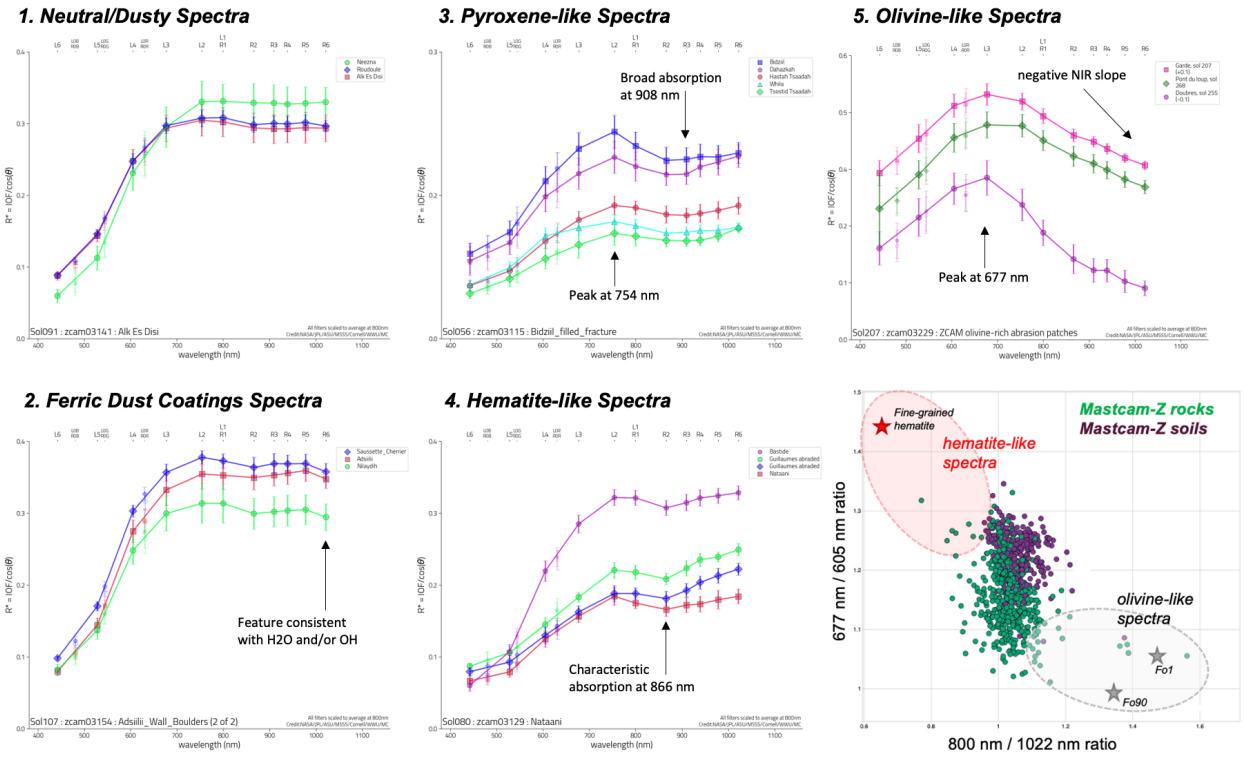

Figure 1. Examples of the main classes of Mastcam-Z spectra and their defining spectral characteristics. Spectra from the left- and right-Mastcam-Zs have been scaled to their average value at 800 nm (L1/R1); broadband (L0/R0) values are shown as small symbols. Error bars show the variance within each ROI, which is generally much larger than the instrumental uncertainty [2]. In the lower right panel, all Mastcam-Z rock (green) and soil (purple) spectra are plotted in a parameter space that distinguishes olivine-like and hematite-like spectra from the rest of the dataset, with the pure laboratory minerals [11] as stars. Mastcam-Z spectra most consistent with hematite are from abraded "paver" rocks; those closest to pure olivine are from abraded rocks in Séítah.

5. Olivine-like Spectra are characterized by weak 528 nm bands, reflectance peaks near 677 nm, and strongly negative near-infrared slopes. These spectra are associated with coarse grained soils encountered early in the traverse on the Cf-fr unit, and with layered rocks in the South Séítah region (where olivine and carbonate minerals have been previously detected from orbit [e.g, 8]). The strongest olivine signatures are seen in the abraded patches and drill tailings on the Bastide and Brac outcrops (targets Garde and Dourbes), where PIXL and SHERLOC observations confirmed the presence of olivine and pyroxenes with some alteration to carbonates and other phases [9]. These targets are spectrally similar to moderately-weathered ultramafic rocks, such as the Twin Sisters dunite [10].

Olivine-like spectra are distinguishable from the rest of the dataset in the parameter space by large 800 nm / 1022 nm ratios and small 677 nm / 605 nm ratios (Fig. 1, lower right). Hematite-like spectra plot in the opposite corner of this same parameter space.

Rock and Soil Spectra Comparisons: Of the five spectral classes above, the soils exhibit mostly neutral/dusty, pyroxene-like and olivine-like spectra. Trends in soil spectral variability along Perseverance's traverse do not mimic the trends observed in adjacent rocks; for example, coarse-grained soils with olivine-like spectra were encountered early in the traverse on the Cf-fr, whereas rocks with olivine-like spectra are largely confined to the Séítah region. These observations have implications for the erosion and transportation of sediment in Jezero crater: olivine-bearing soils – sourced from the layered Séítah outcrops – have most likely been transported from Séítah onto the Cf-fr by aeolian processes.

Acknowledgments: Funding for this work was provided by the NASA Mars-2020 mission.

References: [1] Bell J. F. et al. (2021) *Space Sci. Rev.* 217(1). [2] Hayes A. G. et al. (2021) *Space Sci. Rev.* 217(2). [3] Kinch K. M. et al. (2021) *Space Sci. Rev.* 216(8). [4] Million C. C., et al. (2022) *LSPC*, this meeting. [5] Rice M. S. et al. (2010) *Icarus* 225. [6] Johnson J. R. et al. (2021) *Icarus* 357, 114261. [7] Garczynski B. et al. (2022) *LPSC,* this meeting. [8] Horgan B. N. et al. (2020) *Icarus* 339. [9] Hickman-Lewis K. et al. (2022) *LPSC*, this meeting. [10] Curtis, S. et al. (2022) *LSPC*, this meeting. [11] Kokaly R. F. et al. (2017) *USGS Spectral Library Version 7* 1035(61).